ICESat validation of SRTM C-band digital elevation models

Claudia C. Carabajal[1] and David J. Harding[2]

Received 30 June 2005; revised 18 August 2005; accepted 10 October 2005; published 30 November 2005.

[1] The Geoscience Laser Altimeter System (GLAS) on the Ice, Cloud, and land Elevation Satellite (ICESat) provides a globally-distributed data set well suited for evaluating the vertical accuracy of Shuttle Radar Topography Mission (SRTM) digital elevation models (DEMs). The horizontal error (2.4 ± 7.3 m) and vertical error (0.04 ± 0.13 m per degree of incidence angle) for the ICESat data used are small compared to those for SRTM. Using GLAS echo waveforms we document differences between the SRTM C-band phase center and the highest, centroid, and lowest elevations within ICESat laser footprints in the western United States. In areas of low relief and sparse tree cover, the mean and standard deviation of elevation differences between the ICESat centroid and SRTM are −0.60 ± 3.46 m. The differences are −5.61 ± 15.68 m in high relief, sparse tree cover areas, and −3.53 ± 8.04 m in flat areas with dense tree cover. The largest differences occur in rugged, densely-vegetated regions. **Citation:** Carabajal, C. C., and D. J. Harding (2005), ICESat validation of SRTM C-band digital elevation models, *Geophys. Res. Lett.*, *32*, L22S01, doi:10.1029/2005GL023957.

1. Introduction

[2] Assessment of the quality of Digital Elevation Models (DEMs) is crucial to their appropriate use in land process studies, as inputs to models, and for detection of topographic change. The Ice, Cloud and land Elevation Satellite (ICESat) provides globally-distributed elevation data of high accuracy that is well-suited for evaluating continental DEMs. The Shuttle Radar Topography Mission (SRTM), using a C-band (5.6 cm wavelength) Interferometric Synthetic Aperture Radar (InSAR), has produced the most accurate near-global DEM covering land areas between 56°S and 60°N [*Farr and Kobrick*, 2000; *Rabus et al.*, 2003]. The DEM reports the phase center elevation of C-band radar scattering from vegetation and the ground, released for the United States with a spatial sampling of 1 arc second (approximately 30 m).

[3] ICESat's capability to measure the vertical distribution of vegetation and the underlying ground [*Harding and Carabajal*, 2005] provides a means to assess SRTM accuracy, in particular the amount of C-band microwave penetration into vegetation canopies and elevation biases with respect to the ground. Here we report elevation differences between highest, centroid (distance-weighted average), and lowest detected elevations, derived from the ICESat received echo waveform, and the SRTM phase center as a function of tree cover and topographic relief in a region in the Western United States (WUS) bounded between 39°−50°N and 236°−240°E (Figure 1).

2. Data and Methodology

2.1. SRTM

[4] SRTM, a joint mission conducted by NASA and the National Geospatial-Intelligence Agency (NGA), was flown in February 2000. The C-band InSAR, provided by the Jet Propulsion Laboratory (JPL), acquired data in 225 km swaths, and an X-band InSAR, provided by the German and Italian space agencies, acquired data in 50 km swaths. The data used in this study is the unfinished, research grade C-band product processed at JPL and distributed by the U.S. Geological Survey EROS Data Center.

[5] Data used by the SRTM project for system calibration and accuracy assessment included continental-scale kinematic GPS transects, corner reflector arrays, ocean data takes, NGA and JPL ground control points (GCPs), and NGA DEMs from optical imagery [*Farr and Kobrick*, 2000; *Rabus et al.*, 2003]. Horizontal and vertical accuracies achieved are better than the mission specifications of 20 m (circular error at 90% confidence) and 16 m (linear error at 90% confidence), respectively. Results from all land GCPs for North America yield mean vertical errors of −0.8 ± 8.3 m (and ±8.5 m at 90% confidence) [*Rodriguez et al.*, 2005].

[6] The kinematic GPS road surveys used for accuracy validation are vegetation-free and sample flat to low slope terrain, where the radar phase center should correspond to the ground surface and direct comparison to ground truth is straight forward. In vegetated landscapes, where the phase center is located within the vegetation canopy, and in areas of high relief the accuracy evaluation is more complex. ICESat measurements provide a means to evaluate SRTM results over a broad range of vegetation cover and topographic relief conditions.

2.2. ICESat

[7] ICESat carries a single instrument, the Geoscience Laser Altimeter System (GLAS), which measures the travel time of laser returns from the earth surface along profiles, with a spatial resolution of ∼70 m and an along-track sampling of 172 m. Mission details and data products are described by *Zwally et al.* [2002] and *Schutz et al.* [2005]. Highest, centroid, and lowest detected elevations are derived from the received echo waveform, representing the elevation distribution of 1064 nm laser energy reflected from illuminated surfaces within the GLAS footprint [*Harding and Carabajal*, 2005].

[8] We used the GLA14 elevation products (Land/Canopy elevations) for the Laser 3a observation period collected

[1]NVI Inc., Space Geodesy Laboratory, NASA Goddard Space Flight Center, Greenbelt, Maryland, USA.
[2]Planetary Geodynamics Laboratory, NASA Goddard Space Flight Center, Greenbelt, Maryland, USA.

0094-8276/05/2005GL023957$05.00

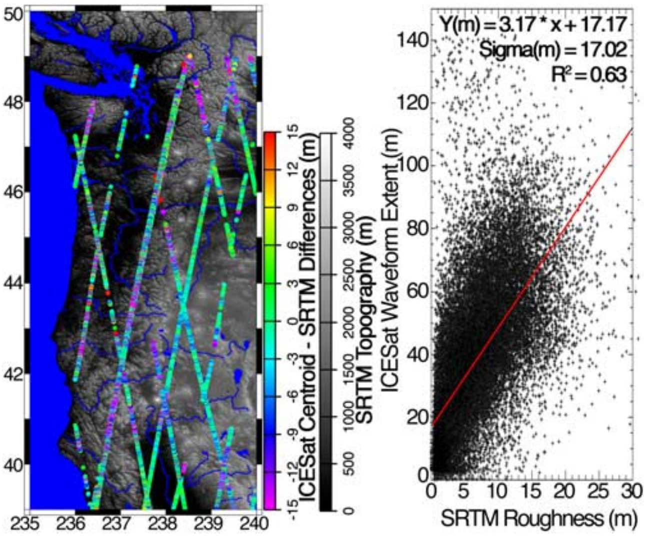

Figure 1. (left) ICESat Laser 3a profiles for the WUS superimposed on gray-scale SRTM topography. Elevation differences greater than ±15 m are plotted as magenta and orange. (right) Relationship between ICESat Waveform Extent and SRTM Terrain ‘‘Roughness’’.

during October–November 2004 and distributed as Release 22 because, at the time of this analysis, that release had the best geolocation accuracy for those periods acquired with a waveform height range of 150 m (minimizing waveform truncation for tall vegetation or steeply sloped ground). Although ‘‘leaf-off’’ foliage conditions comparable to the time of SRTM data acquisition were observed during the Laser 2b and 3b periods in February–March 2003 and 2004, these did not include the latest geolocation calibration corrections and were thus less accurate than the period used. Laser 3a, Release 22 data includes Laser Reference Sensor (LRS) pointing corrections applied to the Instrument Star Tracker (IST) data and the IST field-of-view (FOV) distortion, but not ocean scan nor round the world scan pointing corrections [*Schutz et al.*, 2005].

[9] Pointing errors remaining in the ICESat data translate into horizontal and vertical (elevation) geolocation errors. An estimate of the Laser 3a, Release 22 pointing error based on integrated residual analysis of ocean returns [*Luthcke et al.*, 2000] yields a mean and standard deviation of 0.84 ± 2.5 arc seconds corresponding to a horizontal geolocation error of 2.4 m ± 7.3 m (S. B. Luthcke, personal communication, 2005). The magnitude of the elevation error depends on the incidence angle between the laser vector and the surface normal. For Laser 3a, Release 22, the vertical error is 0.04 ± 0.13 m per degree incidence angle. The nominal 0.3° off-nadir pointing of the laser vector, used to avoid very intense specular reflections from smooth water, translates into a 0.01 ± 0.04 m vertical error for flat surfaces. For sloped surfaces, the elevation error can be negative or positive depending on the azimuths of the pointing error and surface slope. For example, for a 10° surface slope the worst case elevation error due to the mean ± three sigma pointing error ranges between ±4 m.

2.3. Data Comparison

[10] SRTM data are distributed as orthometric elevations with respect to the World Geodetic System WGS 84, using the Earth Gravity Model EGM96 [*Lemoine et al.*, 1998] to convert from ellipsoidal elevations. ICESat GLA14 data contain elevations with respect to the TOPEX/Poseidon-Jason ellipsoid [*Schutz et al.*, 2005]. For comparison to SRTM, we converted ICESat footprint locations to the WGS 84 ellipsoid, and then obtained orthometric elevations by applying the EGM96 geoid, interpolated to each footprint location. We derive ICESat’s highest, centroid, and lowest detected elevations from the alternate land surfaces parameters distributed in the GLA14 data product. We also computed waveform extent (highest elevation – lowest elevation), which is a measure of the combined effects of vegetation height and ground relief within the laser footprint.

[11] For every ICESat footprint, we computed the corresponding SRTM elevation using bilinear interpolation. We obtained a measure of ‘‘SRTM roughness’’ by using the standard deviation of elevations in a 3 × 3 array of posts centered at the footprint location (approximately equivalent to the footprint area). This estimate includes the combined effects of topographic relief, SRTM measurement noise (i.e., post-to-post relative elevation error), and where vegetated, variable C-band microwave penetration into the vegetation cover. In areas of thick cloud cover, either no laser return is detected or it corresponds to the cloud top. We excluded outliers with ICESat centroid minus SRTM differences larger than 100 m, assumed to be returns from

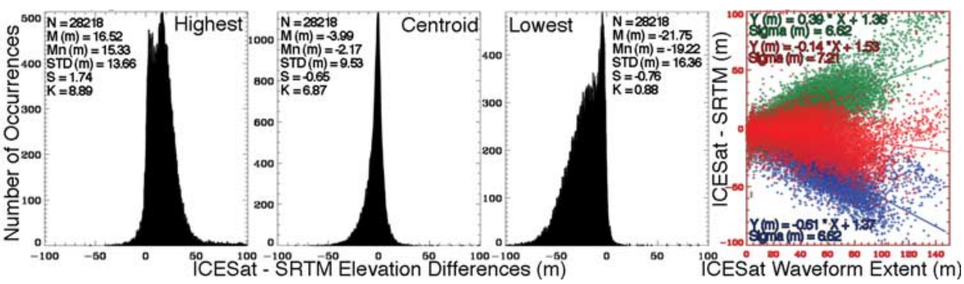

Figure 2. (left) Histograms of highest, centroid, and lowest ICESat minus SRTM elevations for the WUS, and associated statistics (N = Number of Points; M = Mean; Mn = Median; STD = Standard Deviation; S = Skew; K = Kurtosis). (right) Relationship between waveform extent and ICESat minus SRTM elevation differences for the highest (green), centroid (red) and lowest (blue) detected ICESat elevations (excluding outliers). Results of linear regressions applied to the data distributions are shown with same-color solid lines and equations.

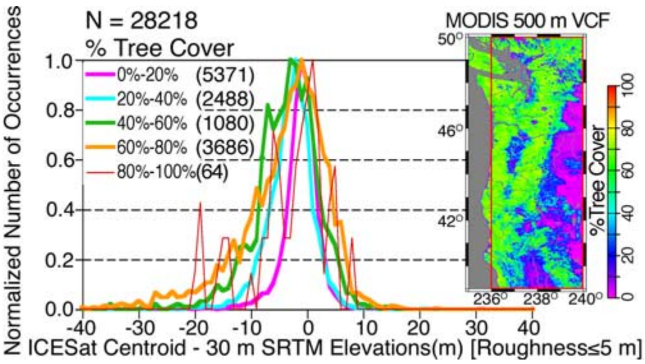

Figure 3. (right) MODIS 500 m VCF % tree cover map for the WUS and (left) normalized histograms of ICESat centroid minus SRTM elevations as a function of % tree cover classes where SRTM roughness is between 0 and 5 m. The number of occurrences, in parentheses, is low for the 80 to 100% class so the distribution is poorly determined.

clouds. Returns with waveforms that were considered to be saturated or truncated [*Harding and Carabajal*, 2005] were also excluded. No editing based on off-nadir pointing was done, but most data included were acquired at the nominal near-nadir pointing.

[12] To evaluate the influence of vegetation cover on SRTM elevation biases, we examined the relationship between % tree cover and ICESat-SRTM elevation differences. We used the aerial proportional estimate of woody vegetation (% tree cover) provided in the 500 m resolution Vegetation Continuous Fields (VCF) product, derived from the Moderate Resolution Imaging Spectroradiometer (MODIS) [*Hansen et al.*, 2003] at every ICESat footprint location. VCF % tree, herbaceous, and bare cover estimates were developed from global training data (representative known pixels that describe the spectral range of every class) derived using high-resolution imagery. *Hansen et al.* [2003] used the training data and phenological metrics, from cloud-corrected monthly composites of MODIS surface reflectance, in a decision tree algorithm to derive % cover globally.

3. Results

[13] Figure 1 (left) shows the geographic distribution of elevation differences (ICESat centroid – SRTM) along Laser 3a profiles for the WUS. Profile gaps are the result of dense cloud cover at the time of the ICESat acquisition or voids in the SRTM data caused by radar shadowing in areas of high relief or areas where InSAR coherence was poor. The correlation between waveform extent and SRTM roughness is linear but exhibits large scatter (Figure 1 (right)). Larger elevation differences, either positive or negative, are associated with areas of greater topographic roughness. The histogram of ICESat centroid minus SRTM elevations is strongly peaked close to zero and symmetrical (Figure 2). The ICESat lowest minus SRTM distribution has a peak at approximately −5 m and a pronounced, negatively skewed tail. The ICESat highest minus SRTM distribution has a peak at approximately 5 m and a larger second peak at 15 m. Nearly all the SRTM elevations occur between the highest and lowest ICESat elevations. The relationship between ICESat-SRTM differences and waveform extent is illustrated in Figure 2 (right); as waveform extent increases, the C-band phase center is, on average, increasingly biased below the ICESat highest elevation and above the ICESat lowest elevation, but is relatively unbiased with respect to the waveform centroid. Distributions of ICESat centroid minus SRTM elevation differences broaden and become more negatively skewed as the proportion of tree cover increases for low SRTM roughness areas (Figure 3).

Table 1. ICESat Minus 30 m SRTM Elevation Differences Classified by % Tree Cover From the 500 m MODIS VCF Product and SRTM "Roughness" (Standard Deviation of Elevations in a 3 × 3 Posts Arrays) Centered at the Geolocated ICESat Footprint

	% Tree Cover Class															
	<20%			20%–40%			40%–60%			60%–80%			80%–100%			
	Elevation Differences															
SRTM "Roughness" Class (m)	Mean (m)	STD (m)	N	Mean (m)	STD (m)	N	Mean (m)	STD (m)	N	Mean (m)	STD (m)	N	Mean (m)	STD (m)	N	NP 27676
	ICESat Centroid—1 Arcsecond SRTM															
≤5	−0.60	3.46	5371	−2.48	4.04	2488	−3.08	5.58	1080	−3.53	8.04	3686	−2.65	6.81	64	12689
5–10	−0.99	8.04	1522	−3.07	7.33	1420	−4.24	8.06	902	−6.23	10.43	4674	−7.38	10.52	80	8598
10–15	−2.17	11.11	618	−4.22	10.67	606	−4.43	10.89	497	−8.63	12.85	2896	−9.38	12.52	41	4658
15–20	−5.61	15.68	214	−4.79	15.44	169	−6.47	13.24	159	−11.18	15.02	811	−12.71	10.77	12	1365
>20	−4.75	22.02	78	−5.53	21.48	52	−7.36	23.98	32	−12.02	21.33	198	−32.93	22.62	6	366
	ICESAT Highest—1 Arcsecond SRTM															
≤5	6.39	6.39	5371	10.76	9.68	2488	13.06	13.02	1080	17.38	13.52	3686	16.52	9.20	64	12689
5–10	15.72	10.36	1522	17.89	11.19	1420	17.85	11.67	902	21.49	13.06	4674	19.85	12.29	80	8598
10–15	21.39	13.73	618	21.48	11.29	606	22.14	12.02	497	25.10	14.18	2896	25.44	11.20	41	4658
15–20	22.73	15.67	214	24.35	15.85	169	22.47	15.62	159	25.93	15.31	811	28.17	16.99	12	1365
>20	26.80	23.19	78	26.74	21.01	52	29.61	24.13	32	29.82	22.64	198	21.77	19.44	6	366
	ICESAT Lowest—1 Arcsecond SRTM															
≤5	−6.06	5.73	5371	−11.54	7.35	2488	−14.77	8.26	1080	−22.59	11.71	3686	−21.83	10.81	64	12689
5–10	−16.52	10.71	1522	−22.06	10.49	1420	−23.81	10.87	902	−31.21	13.95	4674	−31.62	14.46	80	8598
10–15	−24.40	13.60	618	−28.21	13.70	606	−29.03	13.81	497	−37.44	16.06	2896	−40.00	15.62	41	4658
15–20	−31.10	17.89	214	−31.58	16.64	169	−32.90	14.07	159	−41.54	17.80	811	−43.25	12.99	12	1365
>20	−31.42	23.46	78	−32.57	21.89	52	−35.23	25.77	32	−43.79	24.50	198	−73.56	26.77	6	366
NP			7803			4735			2670			12265			203	27676

[14] Elevation difference statistics as a function of % tree cover and SRTM roughness classes (binned at 20% and 5 m increments, respectively) are shown in Table 1. Water covered areas, which do not have VCF proportions reported (542 returns), are excluded. For ICESat centroid minus SRTM elevation differences, the mean bias is negative for all combinations of tree cover and roughness classes. The smallest mean bias occurs over relatively flat areas (SRTM-derived roughness $\leq$5 m) with low tree cover (0 to 20%), which represent 28% of the measurements. The mean bias becomes more negative with increasing tree cover and roughness, except for some class combinations with inconsistent results due to low sample number. The standard deviation is also lowest for the low roughness, sparse tree cover class combination and increases with tree cover and to a lesser degree with roughness, likely due to the imprecision of SRTM values versus the more precise GLAS measurements.

[15] The mean biases for the ICESat highest minus SRTM elevation differences are all positive and become larger with increasing tree cover and roughness, whereas the differences with respect to ICESat lowest elevations are all negatively biased and become more negative with increasing tree cover and roughness. For comparable tree cover and roughness class combinations, the ICESat lowest elevations are further below the SRTM elevation, on average, than the ICESat highest elevations are above the SRTM elevation, becoming more so with increasing tree cover and roughness (Figure 3, histograms, and Table 1). The standard deviations for the highest and lowest elevation differences are comparable in magnitude for each class combination and exhibit similar trends to, but are larger than, those for the centroid differences.

4. Discussion

[16] SRTM elevations closely correspond to the ICESat centroid, indicating that C-band radar scatterers and optical reflectors yield a similar elevation. In areas of sparse tree cover, topographic relief is likely to be the dominant contributor to the SRTM roughness value and it can thus be used as a proxy for relief. The well-defined peaks near zero in the elevation difference distributions are associated with sparsely vegetated, low relief areas that have an ICESat centroid minus SRTM difference of -0.60 ± 3.46 m. This is in close agreement with previous accuracy estimates and well within the SRTM requirement. The tail in the ICESat lowest distribution and the peak centered near 15 m in the ICESat highest distribution are associated with areas of increasing tree cover and/or relief (Figure 2).

[17] SRTM elevations with respect to ICESat's highest-canopy and lowest-ground detected elevations for tree covered, low SRTM roughness areas indicate that C-band radar phase center penetrates slightly less than half way into the canopy on average. With increasing tree cover, the phase center relative to the ground becomes increasingly displaced upward into the canopy as more radar energy is reflected from canopy components and less from the ground, and the variability of the SRTM elevation relative to the highest and lowest surfaces detected by ICESat becomes larger. The increasing upward bias and greater variability make the SRTM elevation an increasingly less reliable measure of ground topography as tree cover increases. Similarly, SRTM elevations become more upward biased and variable relative to the ICESat elevations as relief increases in areas of low tree cover. This increasing upward bias suggests that the radar phase center becomes preferentially more sensitive to higher ground surfaces than does ICESat as relief increases.

[18] Because of ICESat geolocation errors caused by incomplete pointing corrections in Laser 3a, Release 22, the elevation difference standard deviations reported here are probably a slight overestimate. However, the mean biases and trends as a function of tree cover and SRTM roughness should not be affected significantly. Because the nominal laser pointing angle is slightly off-nadir, small elevation biases are introduced in the ICESat data by geographically-correlated pointing errors [*Luthcke et al.*, 2005] but these are at the centimeter- to decimeter-level and are small compared to the ICESat versus SRTM biases. Improved ICESat to SRTM elevation differences will be obtained with later ICESat data releases that include scan maneuver calibrations as they become available.

[19] These results provide a method to estimate SRTM elevation biases and variability with respect to lowest, average, and highest elevations by utilizing the MODIS VCF tree cover estimate, available globally, and SRTM roughness estimates. Thus, the suitability of the SRTM elevation data in studies requiring ground topography can be assessed. Furthermore, in non-vegetated areas the ICESat data can be used to correct SRTM biases. Analyses in Amazonia, and parts of East Africa, the Tibetan Plateau, Himalayan Mountains, and Western Australia demonstrate that the SRTM elevation biases vary from region to region [*Carabajal and Harding*, 2005]. Ultimately, we will perform a global study to comprehensively evaluate SRTM elevation differences with respect to fully calibrated ICESat data, providing a complete assessment of SRTM accuracy.

[20] **Acknowledgments.** This research was supported by NASA's ICESat Project and Solid Earth and Natural Hazards Program (RTOP 622-74-10). We thank the ICESat Science Project and the NSIDC for distribution of the ICESat data (see http://icesat.gsfc.nasa.gov and http://nsidc.org/data/icesat/), the ICESat Science Investigator-led Processing System and Science Computing Facility staff, especially K. Barbieri and J. Guerber, for providing valuable assistance, and S. Luthcke and D. Rowlands for helpful discussions. We thank J. Bufton for his support, and H. Fricker, C. Shuman and R. Schutz and anonymous reviewers for their valuable input.

References

Carabajal, C., and D. Harding (2005), Validation of SRTM C-Band DEMs using ICESat, *Photogramm. Eng. Remote. Sens.*, in press.

Farr, T., and M. Kobrick (2000), Shuttle Radar Topography Mission produces a wealth of data, *Eos Trans. AGU*, *81*, 583–585.

Hansen, M., et al. (2003), Global percent tree cover at a spatial resolution of 500 meters: First results of the MODIS Vegetation Continuous Fields algorithm, *Earth Interact.*, *7*, 1–15.

Harding, D. J., and C. C. Carabajal (2005), ICESat waveform measurements of within-footprint topographic relief and vegetation vertical structure, *Geophys. Res. Lett.*, *32*, L21S10, doi:10.1029/2005GL023471.

Lemoine, F., et al. (1998), The development of the Joint NASA GSFC and NIMA Geopotential Model EGM96, *NASA Tech. Pap., TP-1998–206861*, 575 pp.

Luthcke, S., D. Rowlands, J. McCarthy, D. Pavlis, and E. Stoneking (2000), Spaceborne laser-altimeter-pointing bias calibration from range residual analysis, *J. Spacecr. Rockets*, *37*, 374–384.

Luthcke, S. B., D. D. Rowlands, T. A. Williams, and M. Sirota (2005), Reduction of ICESat systematic geolocation errors and the impact on ice

sheet elevation change detection, *Geophys. Res. Lett.*, *32*, L21S05, doi:10.1029/2005GL023689.
Rabus, B., M. Eineder, A. Roth, and R. Bamler (2003), The Shuttle Radar Topography Mission—A new class of digital elevation models acquired by spaceborne radar, *Photogramm. Remote. Sens.*, *57*, 241–262.
Rodriguez, E., et al. (2005), An Assessment of the SRTM Topographic Products, report, Jet Propul. Lab., Pasadena, Calif.
Schutz, B. E., H. J. Zwally, C. A. Shuman, D. Hancock, and J. P. DiMarzio (2005), Overview of the ICESat Mission, *Geophys. Res. Lett.*, *32*, L21S01, doi:10.1029/2005GL024009.
Zwally, H., et al. (2002), ICESat's laser measurements of polar ice, atmosphere, ocean and land, *J. Geodyn.*, *34*, 405–445.

C. C. Carabajal, Space Geodesy Laboratory, NASA Goddard Space Flight Center, Code 697, Greenbelt, MD 20771, USA. (Claudia@bowie.gsfc.nasa.gov)

D. J. Harding, Planetary Geodynamics Laboratory, NASA Goddard Space Flight Center, Code 698, Greenbelt, MD 20771, USA.